Characterization of Inertance Tubes Using Resonance Effects

M.A. Lewis[1], P.E Bradley[1], R. Radebaugh[1] and Z. H. Gan[1, 2]

[1]National Institute of Standards and Technology
Boulder, CO 80305, USA
[2]Institute of Refrigeration and Cryogenics
Zhejiang University, Hangzhou, 310027, P.R. China

ABSTRACT

Inertance tubes can be characterized by their inertance, compliance, and resistance. All three of these impedance components are present during normal measurements of inertance tube impedance. As a result, in comparing experimental results with models, it is often difficult to find the fundamental cause of disagreement. In previous measurements of inertance tubes we have observed resonance conditions when the reservoir volume is properly sized. The resonance is analogous to an *LC* resonance of electrical systems with *L* analogous to the inertance and C analogous to the compliance of the inertance tube and reservoir volume. This paper discusses how we make use of this resonance to separate the various impedance components of the inertance tube and compare them with models. Frequency is varied about the resonance frequency for fixed pressure amplitude to find the resonance frequency, the minimum impedance, and the half-width of the resonance peak. Other measurements are made with both zero reservoir volume and large reservoir volume. With this set of measurements, we show how to separate the impedance components to compare them with models. Various methods for mass flow measurements at the inlet to the inertance tube are compared. These include hot-wire anemometry, pressure drop across stacked screen, and pressure drop across a laminar flow element. The inertance tubes investigated here are 5.74 mm and 8.71 mm in diameter with lengths of 2.36 and 3.59 meters, respectively. Average pressures range from 1.5 to 2.5 MPa and pressure ratios extend up to 1.3 to give acoustic powers ranging from about 200 to 1500 W. The reservoir volumes are sized to produce resonance frequencies near 60 Hz.

INTRODUCTION

The inertance tube is a component of higher frequency pulse tube cryocoolers, as indicated in Fig. 1. It must be sized correctly so that its flow impedance allows for the proper amplitude and phase of the mass flow rate for a given pressure amplitude. For an optimum design, where the flow and pressure are in phase at the midpoint of the regenerator, the flow at the inlet to the inertance tube must lag the pressure by about 60°.[1] A good model of the inertance tube is required to correctly size it to provide the desired complex flow impedance. Experimental

Cryocoolers 14, edited by S.D. Miller and R.G. Ross, Jr.

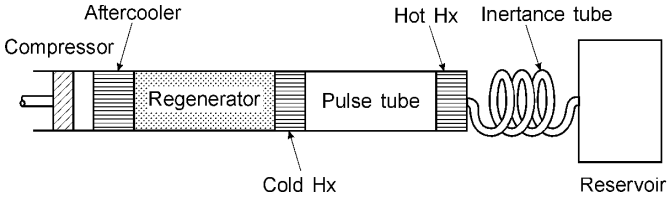

Figure 1. Schematic of pulse tube cryocooler with inertance tube.

measurements are required to verify the accuracy of any inertance tube model. We have used a simple model for the design of inertance tubes that consists of a transmission line analogy.[1] Previous experiments have compared a small inertance tube of 1.57 mm diameter and 1.15 meters in length and a larger inertance tube of 5.74 mm diameter and 2.36 meter in length. The smaller inertance tube showed maximum acoustic power flow values of about 40 W.[2] The larger inertance tube obtained maximum acoustic power flows that vary from 100 W to 800 W.[3] In those experiments various reservoir volumes were used to obtain this wide range of acoustic powers. These techniques have a significant effect on both the magnitude and the phase at the inlet of the inertance tube. For the experiments reported here we have included more test results on the 5.74 mm diameter and 2.36 meter length inertance tube in addition to an 8.71 diameter and 3.59 meter length inertance tube. These experiments used multiple reservoirs as the previous tests had done. These experiments concentrated on obtaining maximum acoustic power flows using various reservoir volumes by adjusting the frequency of the oscillating flow at a specific operating pressure ratio or mass flow rate. Large acoustic power flows were obtained as a result of smaller reservoir volumes. When using the 83 cm^3 reservoir volume we obtained the largest range of pressure ratios for both inertance tubes. Measured values on the peak acoustic power for the 5.74 mm diameter inertance tube at a pressure ratio of 1.30 was about 880 W at 58 Hz and that for the 8.71 mm diameter inertance tube at a lower pressure ratio of 1.07 was about 316 W at 56 Hz.

TRANSMISSION LINE MODEL

For fluid systems, the impedance is

$$\text{(Fluid)} \quad Z = \boldsymbol{P}/\dot{\boldsymbol{V}} = \rho_0 \boldsymbol{P}/\dot{\boldsymbol{m}} = \rho_0 Z_m, \tag{1}$$

where $\boldsymbol{P}$ is the dynamic pressure, $\dot{\boldsymbol{V}}$ is the volume flow rate, and Z_m is the impedance to mass flow. We prefer the use of Z_m because mass flow is conserved, whereas volume flow is not. For the fluid transmission line the resistance, inertance, and compliance per unit length appropriate to Z_m are:[1]

$$\text{(resistance/length)} \quad r(D) = \left[\frac{32 f_r |\dot{\mathbf{m}}|}{\pi^2 \rho_0 D^5}\right], \tag{2}$$

$$\text{(inertance/length)} \quad \ell(D) = 4/(\pi D^2), \tag{3}$$

$$\text{(compliance/length)} \quad c(D) = (\pi D^2)/(4\gamma R T_0), \tag{4}$$

where D is the tube inner diameter, f_r is the Fanning friction factor, γ is the ratio of specific heats, R is the gas constant per unit mass, and T_0 is the temperature of the helium gas. Some calculations are made with a factor of $2/\pi$ to give a resistance to the average mass flow in one half cycle. This factor does not provide good agreement with the experimental results. They are indicated by thin lines in some of the graphs shown later. The inclusion of γ in equation (4) implies an adiabatic process, although it could be varied between 1.0 and 1.67 to allow for any heat transfer intermediate between isothermal and adiabatic. The incorporation of the friction factor in equation (2) allows the use of this model in both the laminar and turbulent flow regions. We also take into account surface

roughness in the calculation of the friction factor, and for the calculations given here we assumed a surface roughness inside the inertance tube of 1.0 μm. Steady-state correlations [4] for tubes are used for the friction factor rather than any complex oscillating flow correlation. There certainly is some question whether such a steady-state correlation is valid for oscillating flow, particularly for the large tube used here, where the ratio of tube radius to viscous penetration depth varies from 15 to 20, and the peak Reynolds numbers are about 1×10^5. Turbulence models [5] for oscillating flow with conditions similar to that experienced here suggest steady-state correlations are valid. Indeed, the purpose of the experiments being reported here is to evaluate the validity of the simple transmission line model with steady-flow correlations for larger inertance tubes.

The reservoir of volume V_r at the end of the inertance tube introduces a compliant load on the end of the fluid transmission line of

$$C_r = V_r /(\gamma R T_r). \tag{5}$$

The impedance of this compliant load is

$$Z_r = 1/(i\omega C_r). \tag{6}$$

The complex impedance of a terminated transmission line is defined in previous inertance tube experiments and published documents. [3, 6, 7]

EXPERIMENTAL PROCEDURE

Mass flow measurement methods

The test apparatus was designed to obtain mass flow measurements at the outlet of a 2.8 kW commercial linear compressor. This would allow the mass flow information to be obtained at the inlet of the inertance tube once it was installed onto the test apparatus. At the compressor outlet an aftercooler was installed that consisted of a set of copper stacked screens that were sandwiched around copper tubing. The copper tubing allowed water flow cooling at the compressor outlet. Mounted to the aftercooler was a hot wire housing that consisted of two hot wires mounted at the center of the flow. On each side of this housing were stacked screens to provide uniform flow profiles for the hot wire measurements and to protect the hot wire from damage due to particles in the flow stream. Connected to the hot wire housing was a 155 cm^3 reservoir volume. At the reservoir both piezoresistive and piezoelectric pressure transducers were installed. Platinum resistor thermometers were mounted in various locations to measure the temperature as required. The compressor was operated to provide specific pressure ratio values at the hot wire inlet. Once the inlet pressure ratios were set, the pressure and temperature measurements could be made at the reservoir volume and mass flow calculations made by use of the following equation

$$\dot{m}_r = \frac{\dot{P} V_r}{\gamma R T_r}, \tag{7}$$

where $\dot{P}$ is the time derivative of the pressure, V_r is the reservoir volume, and T_r is the reservoir temperature. Measurements for mass flow were also made simultaneously using the differential pressure at the aftercooler and hot wire housing, as well as the output voltages of the two anemometers. These series of measurements provided calibration data values to be used for measuring mass flow at this location, which would eventually be the inlet inertance tube location. From these calibration results the hot wire calibrations were used, as well as the differential pressure measurements across the hot wire housing. The differential pressure measurements across the aftercooler were much lower values than those of the hot wire housing, so these were not used to calculate mass flow. The calibration data were taken from pressure ratios of 1.05 to 1.35, frequencies of 40 to 70 Hz, and pressures of 1.5, 2.0 and 2.5 MPa. The hot wire data showed no dependences on frequency or pressure. The differential pressure measurements showed pressure dependences. Specific curve fit data needed to be applied depending on the operating pressure.

Measurement Methods

The measurements were taken on two inertance tubes with inside diameters of 5.74 and 8.71 mm and lengths of 2.36 and 3.59 meters, respectively. The measurements were made by connecting a reservoir volume directly to the hot-wire anemometer and differential pressure flowmeter without the inertance tube in place. In that case the flow at the inlet to the reservoir, given by equation (7), is the same as that through the flowmeter. Once the flowmeter calibrations were completed, the 155 cm^3 mass flow calibration reservoir volume was removed. The individual inertance tubes were connected directly downstream of the flowmeter. The other end of each inertance tube was connected to a manifold where there were four other reservoir volumes attached. The manifold and respective reservoirs allowed experimental data to be taken on these separate reservoir volumes at the exit of the inertance tubes. These reservoir volumes were 30, 83, 134 and 334 cm^3. The three largest reservoir volumes had piezoresistive transducers and the smallest reservoir volume had both piezoresistive and piezoelectric transducers for accurate measurements of pressure amplitude. All reservoir volumes as well as the inertance tube were instrumented with temperature sensors. Cooling air was supplied to maintain temperature control and prevent overheating of the reservoir volumes when high acoustic power flow was measured.

The pressure amplitudes and phase angles were measured with lock-in amplifiers. The hot-wire anemometers were made of tungsten wire with a diameter of 3.8 μm and had specific instrumentation to measure and calculate the voltage output, as required.

EXPERIMENTAL RESULTS

Experimental data were recorded to calculate the acoustic power flows at specific pressure ratios. The test plan measured this acoustic power flow over a range of frequencies generated by the power supply to observe the maximum power obtained at a given frequency. It also included data on both side of the maximum frequency to plot a bell-shaped curve of the acoustic power when possible. The output power from the power supply had limitations that prevented obtaining data at certain ranges for each pressure ratio when the current levels became too high. Figures 2, 3, 4 and 5 show the results of these acoustic measurements for the 5.74 mm diameter inertance tube. Many of the results are compared with the transmission line model data, as in Figure 2. The calculated model results are compared to the acoustic power flows calculated at a pressure ratio of 1.07 and a reservoir volume of 30 cm^3. The model shows a lower frequency and acoustic power than the experimental data at the maximum acoustic power obtained.

The lower resonance frequency from the model indicates the *lc* product from the model, equation 3 and 4, is somewhat higher than the experimental value. The value of peak acoustic

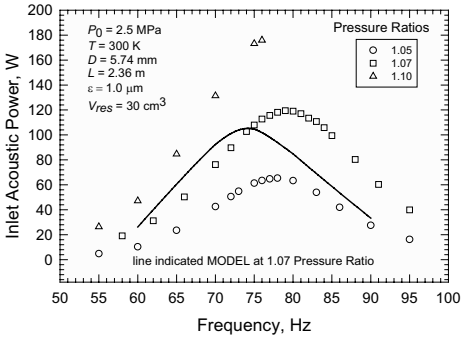

Figure 2. Inlet acoustic power vs. frequency for a reservoir volume of 30 cm^3

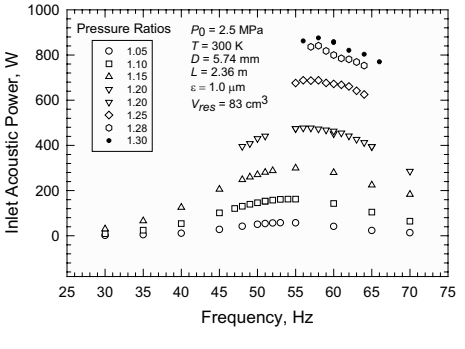

Figure 3. Inlet acoustic power vs. frequency for a reservoir volume of 83 cm^3

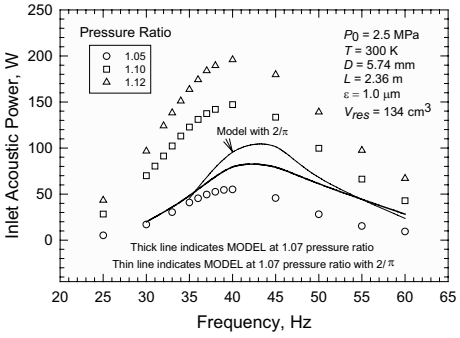

Figure 4. Inlet acoustic power vs. frequency for a reservoir volume of 134 cm^3

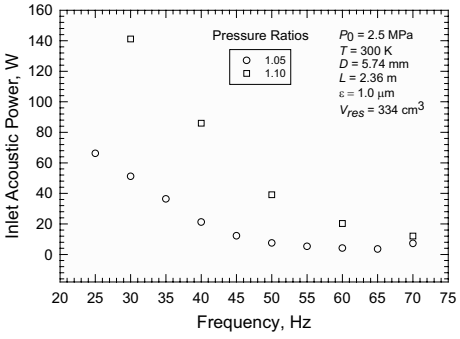

Figure 5. Inlet acoustic power vs. frequency for a reservoir volume of 334 cm^3

power is proportional to the inverse of the resistive component, whereas the half-width of the resonance curve is proportional to the resistive component. Figure 2 indicates good agreement between the model and the experimental results for both the peak and the half-width, which suggests good agreement for the resistive component.

Figure 4 and Figure 5 show the acoustic power using the 134 cm^3 and 334 cm^3 reservoir volume; for the 134 cm^3 reservoir the results are compared to the model data using a pressure ratio of 1.07 from the transmission line model. The experimental data have pressure ratios of 1.05, 1.10 and 1.12 and the model data are in good agreement where the 1.07 experimental pressure ratio data would lie on the plot. The experimental data on the 334 cm^3 reservoir volume were limited due to the power supply current and would have required a frequency of about 10 Hz to reach a peak maximum acoustic power. The experimental data obtained show the increase of acoustic power with lower frequency values and the trend of a low frequency value of about 10 Hz at the peak acoustic power.

Figure 6 and Figure 7 show the experimental results for the 8.71 mm diameter inertance tube for the 30 cm^3 and 83 cm^3 reservoirs, respectively. In Figure 6, the experimental results are taken at pressure ratios of 1.03, 1.05 and 1.20 and compared to the model data at a pressure ratio of 1.05. The experimental data show a higher frequency value at the maximum peak acoustic power than the model for both cases, with or without using 2/π value in the calculation of the average or amplitude of the mass flow measurement. In Figure 7 the experimental data were taken at pressure ratios of 1.03, 1.05 and 1.07, and there are no transmission line model data comparisons shown. In both figures the experimental data show that the pressure ratio has a small effect on the frequency values where the maximum acoustic power is obtained.

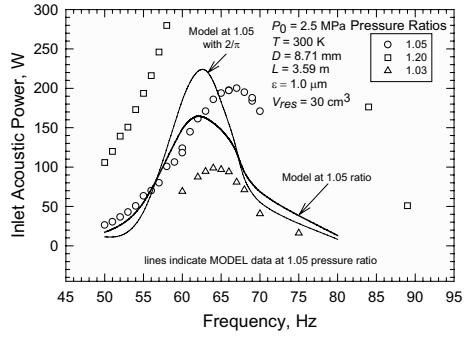

Figure 6. Inlet acoustic power vs. frequency for a reservoir volume of 30 cm^3

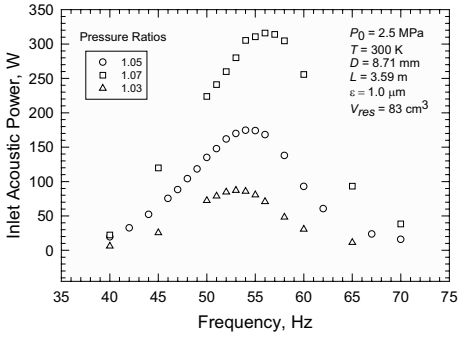

Figure 7. Inlet acoustic power vs. frequency for a reservoir volume of 83 cm^3

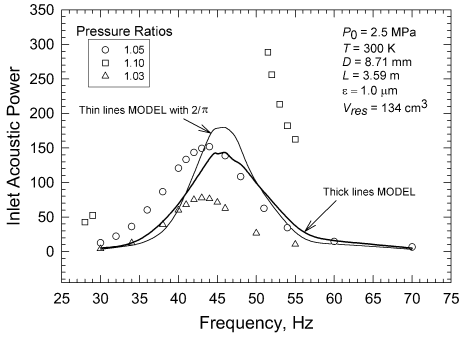

Figure 8. Inlet acoustic power vs. frequency for a reservoir volume of 134 cm^3

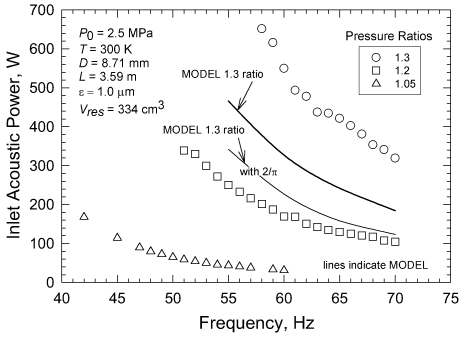

Figure 9. Inlet acoustic power vs. frequency for a reservoir volume of 334 cm^3

In Figure 8 and Figure 9 the experimental acoustic power values are give for the 8.71 mm diameter inertance tube for the 134 cm^3 and 334 cm^3 reservoir volumes. Figure 8 shows experimental data at pressure ratios of 1.03, 1.05 and 1.10 and transmission line model data at a pressure ratio of 1.05 with and without the 2/π value for mass flow calculations. The model data are in good agreement with the experimental data, particularly when calculating the mass flow using the amplitude of the mass flow value, without using the 2/π. Figure 9 shows experimental data at pressure ratios of 1.05, 1.20 and 1.30 and transmission line model data at a pressure ration of 1.30. The frequency at the peak acoustic value was not obtained, but the tendencies indicate an increasing acoustic power at continued lower frequencies and that the frequency value at the peak acoustic power would be a low frequency of about 10-20 Hz. The model data show good agreement of the curve shape and without using the 2/π comparison.

The results of the acoustic power flow experiments are also listed in tabulated form for reservoir sizes of 30, 83 and 134 cm^3. The peak values are shown in Table 1 for the 5.74 mm diameter and 2.36 meter length inertance tube. The peak acoustic power frequency decreases with the reservoir volume size. The experimental data show these values to be about 80 Hz at 30 cm^3, 57 Hz at 83 cm^3, and 40 Hz at 134 cm^3. The phase between the pressure and the flow should approach zero degrees at resonance, and the experimental data indicate this value. Table 2 shows the peak values of acoustic power for the three reservoirs on the 8.71 mm diameter and 3.59 meter length inertance tube. The peak acoustic power decreases with reservoir volume size, with the frequency value being about 68 Hz at 30 cm^3, 55 Hz at 83 cm^3, and 44 Hz at 134 cm^3. The phase angle between the pressure and flow approaches zero degrees at the peak conditions. The experimental peak values

Table 1. Inertance Tube 5.74 mm diameter and 2.36 meter length

Reservoir Volume cm^3	Pressure Ratio	Peak Acoustic Power, W	Peak Frequency, Hz	Peak Impedance MPa·s/kg	Phase Pressure-Flow, degrees
30	1.05	65.4	78	7.50	-4.16
30	1.07	119.4	79	8.51	-5.25
30	1.10	190	80	9.0	-5.55
83	1.05	59.8	54	8.34	-4.26
83	1.10	162.5	55	10.73	-2.30
83	1.15	299.7	55	12.21	-3.36
83	1.20	477.3	56	13.63	-3.77
83	1.25	688.2	56	14.64	-3.22
83	1.28	840.9	58	15.40	-3.19
83	1.30	875.5	58	15.95	0.8
134	1.05	54.95	40	8.88	-4.93
134	1.07	147.20	40	11.43	-5.32
134	1.10	195.80	40	12.22	-5.74

Table 2. Inertance Tube 8.71 mm diameter and 3.59 meter length.

Reservoir Volume cm^3	Pressure Ratio	Peak Acoustic Power, W	Peak Frequency, Hz	Peak Impedance MPa's/kg	Phase Pressure-Flow, degrees
30	1.03	98.7	64	2.28	-5.51
30	1.05	200.2	67	2.67	-0.38
30	1.20	?	70 ?	?	?
83	1.03	87.2	53	2.52	-3.90
83	1.05	174.6	54	2.92	-5.83
83	1.07	316.0	56	3.33	-5.22
134	1.03	77.7	43	2.82	-4.83
134	1.05	151.6	44	3.31	-1.80
134	1.10	?	45 ?	?	?

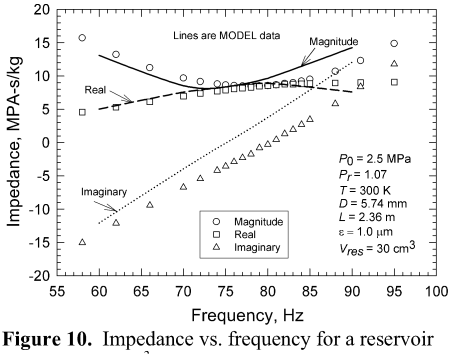

Figure 10. Impedance vs. frequency for a reservoir volume of 30 cm^3

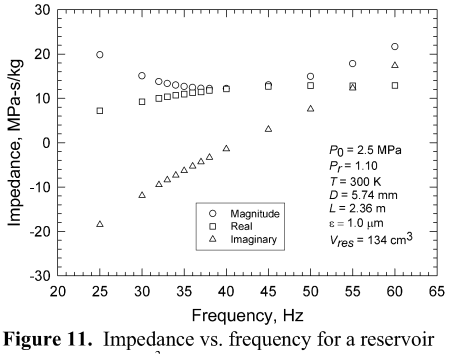

Figure 11. Impedance vs. frequency for a reservoir volume of 134 cm^3

were not obtained at some of the higher pressure ratios because of electrical input power limitations and low frequency requirements. These are indicted by a question mark in the table.

In Figure 10 and Figure 11 the magnitude of the impedance and its relationship to frequency for the 5.74 mm inertance tube are illustrated. The values for the real and imaginary impedance are also shown on both plots. The real values of the impedance are related to the resistive components and have little frequency dependence. The imaginary impedance is dependent on the frequency and has negative values (compliance) at low frequencies but increases to positive values (inertance) at the higher frequency range. In Figure 10 the magnitude, real, and imaginary values are shown from the transmission model data. There is good agreement with both the magnitude and real components, but the imaginary component is lower for the experimental results, particularly at high frequencies. The curve shapes for both plots are quite similar for both the 30 cm^3 and 134 cm^3 reservoir volumes. This behavior is consistent with that determined from a comparison of the reservoir curve in Figure 2.

Figures 12, 13, 14 and 15 show the experimental impedance values for the 8.71 mm and 3.59 m inertance tube for all four volumes and include model data in Figures 12, 14 and 15. In all model cases there is good agreement in the magnitude and real values, but the imaginary value shows separation at frequency values above 60 Hz. The results for both inertance tubes with the largest reservoir volume of 334 cm^3 were unable to reach resonance because of frequency and electrical power input limitations. Figure 15 shows model and experimental data at frequencies from 55 to70 Hz only.

CONCLUSIONS

The experimental data are in good agreement with the model data in most regions. The resonant frequency between the model data and the experimental agree well and should be a function of the inertance and compliance components. Pressure ratio and charging pressure had small effects on

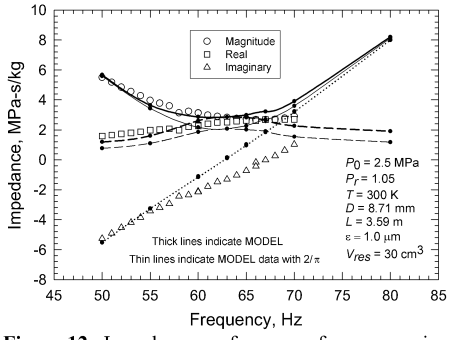

Figure 12. Impedance vs. frequency for a reservoir volume of 30 cm^3

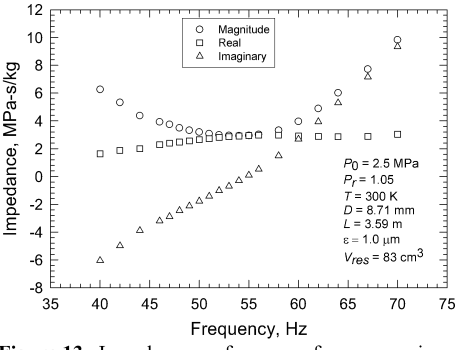

Figure 13. Impedance vs. frequency for a reservoir volume of 83 cm^3

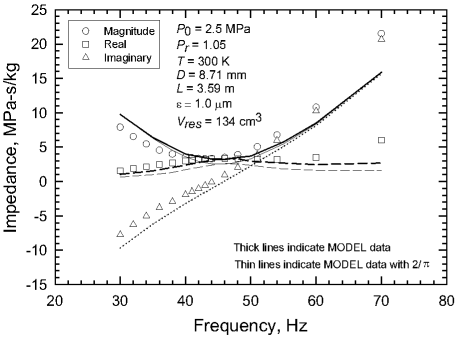

Figure 14. Impedance vs. frequency for a reservoir volume of 134 cm^3

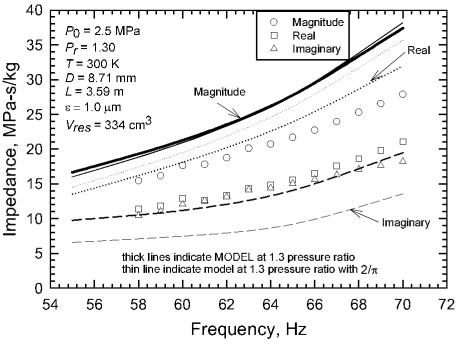

Figure 15. Impedance vs. frequency for a reservoir volume of 334 cm^3

the frequency values at the peak acoustic power flows tested. Improvements are needed in the model for the imaginary component in the high frequency range. Our model is predicting larger imaginary impedance at these higher frequencies when the reservoir volume is small.

REFERENCES

1. Radebaugh, R., Lewis, M., Luo, E., Pfotenhauer, J. M., Nellis, G. F., and Schunk, L. A., "Inertance Tube Optimization for Pulse Tube Refrigerators," *Advances in Cryogenic Engineering*, Vol. 51, American Institute of Physics, 2006, pp. 59-67.

2. Lewis, M. A., Bradley, P. E., Radebaugh, R., and Luo, E., "Measurements of Phase Shifts in an Inertance Tube," *Cryocoolers 13*, Springer, New York, 2004, pp. 267-273.

3. Lewis, M. A., Bradley, P. E., and Radebaugh, R., "Impedance Measurements of Inertance Tubes," *Advances in Cryogenic Engineering*, Vol. 51B, American Institute of Physics, 2006, pp. 1557-1563.

4. Kays, W. M., and London, A. L., *Compact Heat Exchangers*, 3rd edition, McGraw-Hill, New York, 1984.

5. Koehler, W.J., Patanker, S.V., and Ibele, W.E., "Numerical Prediction of Turbulent Oscillating Flow in a Circular Pipe," *Proc. 25th IECEC*, 1990, pp. 398-406.

6. Magnusson, P. C., *Transmission Lines and Wave Propagation*, 2nd edition, Allyn and Bacon, Boston (1970).

7. Skilling, H. H., *Electric Transmission Lines*, McGraw-Hill, New York (1951).